

# Sensorless Speed Control of Asynchronous Motor Using Sliding Mode Observer

*Nguyen Huy Phuong*

*Hanoi University of Science and Technology, No. 1, Dai Co Viet, Hai Ba Trung, Hanoi, Viet Nam*

*Received: May 14, 2019; Accepted: June 24, 2019*

## Abstract

*The application of speed observer instead of direct speed sensor helps asynchronous motor drive reduce cost and improve reliability. The information required for rotor speed estimation is extracted from measured stator voltages and currents at the motor terminals. Different speed estimation algorithms are used for this purpose. The paper concentrates on the design of sliding mode observer for estimating rotor speed in asynchronous motor drive. After general introduction of field-oriented control method for asynchronous motor using voltage source inverter without speed sensor, the paper concentrates on a calculating method of rotor speed using Sliding Mode Observer. In order to confirm the proposed estimation method, an experimental setup of asynchronous motor drive has been built. The experiment results show that the asynchronous motor drive with sensorless field-oriented control strategy works stably in all conditions.*

Keywords: ASM, IM, Sliding Mode Observer, Sensorless Control, Sensorless Drives

## 1. Introduction

With outstanding advantages such as compact, being easy to fabricate, low cost, stability and reliability... the squirrel cage synchronous motor (ASM) is widely used in many industries. However, the ASM drives with precise speed and torque control often require to use relatively expensive speed sensors to provide accurate information on rotor speed and position. In addition, these sensors are often quite sensitive to humidity, temperature, electromagnetic interference and mechanical fluctuations ... thus the stability and reliability of the system will be reduced. To increase the system stability and reduce the cost, the removal of the rotation speed sensor is very important.

In recent years, there are many studies on eliminate the speed sensors from the ASM drives. The popular methods for rotor speed estimation are conducted from measured stator voltages and currents at the motor terminals. These methods are classified according to the algorithm used to estimate the speed.

The most basic method is the Model Reference Adaptive System (MRAS), in which the difference between the measured and estimated variables is used for adaptive adjustment algorithms to give the rotor information [1-3]. The main advantage of this method is stability, rapid convergence and low computational mass. However, the main disadvantage of this method is the sensitivity to the accuracy of the reference

model. In addition, the design of adaptive algorithms is also very complicated due to the requirement of fast response and high stability against noise and disturbances.

To eliminate the effect of noise and disturbances affecting to the system, another method is Kalman filter [4-6]. Kalman filter (KF) algorithm is suitable to the system which has many unknown noises such as current ripple by PWM, noise by modeling error, measurement error, and so forth. Those noises are treated as a disturbance in Kalman filter algorithm. However, this method often requires a large and complex calculation. Moreover, the lack of design standards and tuning criteria is also a problem to developer.

The methods of using artificial intelligence to estimate speed have also been studied in recent times [7-9]. They can approximate a wide range of nonlinear functions to any desired degree of accuracy. Moreover, they have the advantages of immunity from input harmonic ripples and robustness to parameter variations. However, these methods are relatively complicated and require large amount of calculation.

Another method that many scientists are interested in is using Sliding Mode Observers (SMO) to estimate speed [10-12]. The SMO is based on the variable structure control theory which offers many good properties, such as good performance against un-modeled dynamics, insensitivity to parameter variations, external disturbance rejection and fast dynamic response. These advantages are essential for

---

\* Corresponding author: Tel.: (+84) 983088599  
Email: Phuong.nguyenhuy@hust.edu.vn

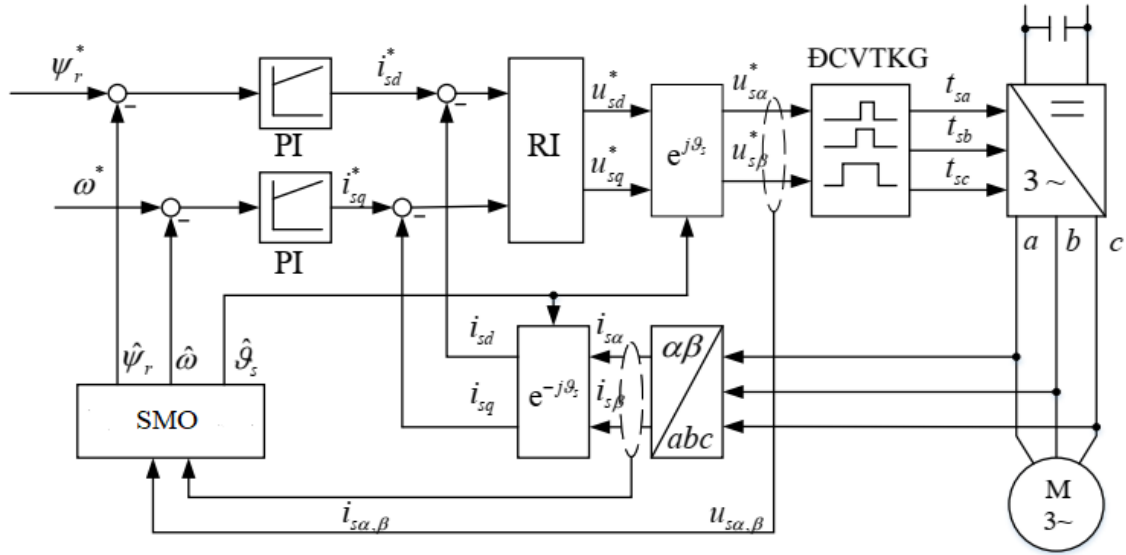


Fig. 1. Sensorless speed control structure of the ASM with sliding mode observer.

estimating the speed of nonlinear plant such as asynchronous motor drives.

Along with the direction on the application of sliding mode control theory, this paper will present a method of estimating the rotation speed based on the model of the motor and the sliding mode control algorithm. To demonstrate the proposed method, both simulation and experimental models are built.

## 2. Sensorless speed control of the ASM

Figure 1 shows a rotor field-oriented control structure of the ASM using voltage source inverter without a speed sensor. Basically this structure is like the classic FOC control structure presented in [14]. The only major difference here is that the speed, position and magnetic flux of the rotor are determined through calculation by the SMO in fixed stator coordinates. Where, the real axis  $\alpha$  coincides with the axis of stator coil  $a$  and the virtual axis is axis  $\beta$ .

### 2.1 Speed estimation using SMO

Information of rotor speed is determined by SMO (Fig. 2) through induced electromotive force with the help of instantaneous values of current and phase voltage as well as motor parameters. Structurally, the sliding mode observer is similar to other observers, the only difference is that the feedback signal is the sign of the error between the calculated and measured currents in the fixed coordinate system.

The state space model of the ASM in the stator fixed frame can be written as [14]:

$$\frac{dx}{dt} = \mathbf{Ax} + \mathbf{Bu} \quad (1)$$

in which:

$$\mathbf{A} = \begin{bmatrix} \mathbf{A}_{11} & \mathbf{A}_{12} \\ \mathbf{A}_{21} & \mathbf{A}_{22} \end{bmatrix}, \mathbf{B} = \begin{bmatrix} \mathbf{B}_1 \\ 0 \end{bmatrix}, \mathbf{I} = \begin{bmatrix} 1 & 0 \\ 0 & 1 \end{bmatrix}, \mathbf{J} = \begin{bmatrix} 0 & -1 \\ 1 & 0 \end{bmatrix}$$

$$\mathbf{A}_{11} = a\mathbf{I}, \mathbf{A}_{12} = c\mathbf{I} - d\mathbf{J}, \mathbf{A}_{21} = e\mathbf{I}, \mathbf{A}_{22} = -\varepsilon\mathbf{A}_{12}, \mathbf{B}_1 = b_1\mathbf{I}$$

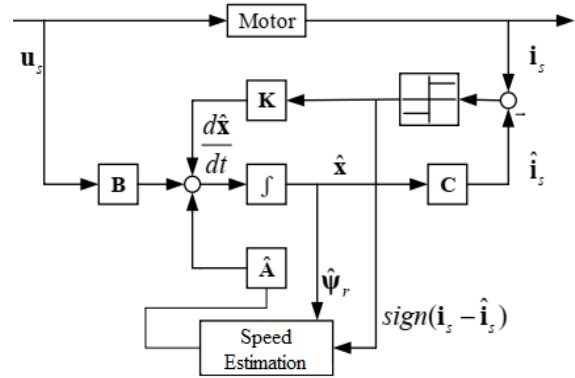


Fig. 2. Sliding mode observer for speed estimation.

$$a = -\left(\frac{R_s}{\sigma L_s} + \frac{L_m^2 \sigma_r}{\sigma L_s L_r}\right), c = \frac{\sigma_r}{\varepsilon}, d = \frac{\omega}{\varepsilon}, e = \sigma_r L_m$$

$$\varepsilon = \frac{\sigma L_s L_r}{L_m}, b_1 = \frac{1}{\sigma L_s}, \sigma = 1 - \frac{L_m^2}{L_s L_r}, \sigma_r = \frac{R_r}{L_r}$$

From the ASM model, the state space model of the SMO can be constructed as:

$$\frac{d\hat{\mathbf{x}}}{dt} = \hat{\mathbf{A}}\hat{\mathbf{x}} + \mathbf{B}\mathbf{u}_s + \mathbf{K}_1 \text{sign}(\mathbf{i}_s - \hat{\mathbf{i}}_s) \quad (2)$$

where  $\mathbf{K}$  is gain matrix which can be arranged in the following general form:

$$\mathbf{K} = \begin{bmatrix} \mathbf{K}_1 \\ -L\mathbf{K}_1 \end{bmatrix}, \mathbf{K}_1 = \begin{bmatrix} k_1 & 0 \\ 0 & k_1 \end{bmatrix}, \mathbf{L} = \begin{bmatrix} l_{11} & l_{12} \\ l_{21} & l_{22} \end{bmatrix} \quad (3)$$

The error state can be defined as:

$$\begin{cases} \mathbf{e} = \mathbf{x} - \hat{\mathbf{x}} = [\mathbf{e}_i & \mathbf{e}_\psi]^T; \\ \mathbf{e}_i = \mathbf{i}_s - \hat{\mathbf{i}}_s; \mathbf{e}_\psi = \boldsymbol{\psi}_r - \hat{\boldsymbol{\psi}}_r \end{cases} \quad (4)$$

The error equation which takes in to account the parameter variation can be expressed by subtracting (1) from (2):

$$\frac{d\mathbf{e}}{dt} = \mathbf{A}\mathbf{e} + \Delta\mathbf{A}\hat{\mathbf{x}} + \mathbf{K}_1 \text{sign}(\mathbf{i}_s - \hat{\mathbf{i}}_s) \quad (5)$$

or:

$$\begin{bmatrix} \frac{d\mathbf{e}_i}{dt} \\ \frac{d\mathbf{e}_\psi}{dt} \end{bmatrix} = \begin{bmatrix} \mathbf{A}_{11} & \mathbf{A}_{12} \\ \mathbf{A}_{21} & \mathbf{A}_{22} \end{bmatrix} \begin{bmatrix} \mathbf{e}_i \\ \mathbf{e}_\psi \end{bmatrix} + \begin{bmatrix} \Delta\mathbf{A}_{11} & \Delta\mathbf{A}_{12} \\ \Delta\mathbf{A}_{21} & \Delta\mathbf{A}_{22} \end{bmatrix} \begin{bmatrix} \hat{\mathbf{i}}_s \\ \hat{\boldsymbol{\psi}}_r \end{bmatrix} + \begin{bmatrix} \mathbf{K}_1 \\ -L\mathbf{K}_1 \end{bmatrix} \text{sign}(\mathbf{i}_s - \hat{\mathbf{i}}_s) \quad (6)$$

where:

$$\Delta\mathbf{A} = \mathbf{A} - \hat{\mathbf{A}} = \begin{bmatrix} \Delta\mathbf{A}_{11} & \Delta\mathbf{A}_{12} \\ \Delta\mathbf{A}_{21} & \Delta\mathbf{A}_{22} \end{bmatrix} = \begin{bmatrix} 0 & -\frac{\Delta\omega\mathbf{J}}{\varepsilon} \\ 0 & \Delta\omega\mathbf{J} \end{bmatrix} \quad (7)$$

$$\Delta\omega = \omega - \hat{\omega}$$

Equation (6), yields:

$$\begin{cases} \frac{d\mathbf{e}_i}{dt} = \mathbf{A}_{11}\mathbf{e}_i + \mathbf{A}_{12}\mathbf{e}_\psi + \Delta\mathbf{A}_{11}\hat{\mathbf{i}}_s + \Delta\mathbf{A}_{12}\hat{\boldsymbol{\psi}}_r + \mathbf{K}_1 \text{sign}(\mathbf{i}_s - \hat{\mathbf{i}}_s) \\ \frac{d\mathbf{e}_\psi}{dt} = \mathbf{A}_{21}\mathbf{e}_i + \mathbf{A}_{22}\mathbf{e}_\psi + \Delta\mathbf{A}_{21}\hat{\mathbf{i}}_s + \Delta\mathbf{A}_{22}\hat{\boldsymbol{\psi}}_r - L\mathbf{K}_1 \text{sign}(\mathbf{i}_s - \hat{\mathbf{i}}_s) \end{cases} \quad (8)$$

Defining the switching surface  $S$  of the SMO as:

$$\mathbf{S}(\mathbf{t}) = \mathbf{e}_i = \mathbf{i}_s - \hat{\mathbf{i}}_s = 0 \quad (9)$$

The sliding mode occurs when the following sliding condition is satisfied:

$$\mathbf{e}_i^T \cdot \frac{d\mathbf{e}_i}{dt} < 0 \quad (10)$$

Since the sliding mode condition is satisfied with a small switching gain, then:

$$\mathbf{e}_i = \frac{d\mathbf{e}_i}{dt} = 0 \quad (11)$$

Then from (8) and (11) we have:

$$\begin{cases} 0 = \mathbf{A}_{12}\mathbf{e}_\psi + \Delta\mathbf{A}_{11}\hat{\mathbf{i}}_s + \Delta\mathbf{A}_{12}\hat{\boldsymbol{\psi}}_r - \mathbf{z} \\ \frac{d\mathbf{e}_\psi}{dt} = \mathbf{A}_{22}\mathbf{e}_\psi + \Delta\mathbf{A}_{21}\hat{\mathbf{i}}_s + \Delta\mathbf{A}_{22}\hat{\boldsymbol{\psi}}_r + L\mathbf{z} \\ \mathbf{z} = -\mathbf{K}_1 \text{sign}(\mathbf{i}_s - \hat{\mathbf{i}}_s) \end{cases} \quad (12)$$

From (12), the error equation for the rotor flux in sliding mode condition is obtained as:

$$\frac{d\mathbf{e}_\psi}{dt} = (\mathbf{A}_{22} + L\mathbf{A}_{12})\mathbf{e}_\psi + (\Delta\mathbf{A}_{21} + L\Delta\mathbf{A}_{11})\hat{\mathbf{i}}_s + (\Delta\mathbf{A}_{22} + L\Delta\mathbf{A}_{12})\hat{\boldsymbol{\psi}}_r \quad (13)$$

Because of  $\Delta\mathbf{A}_{11} = \Delta\mathbf{A}_{21} = 0$  so the error equation for the rotor flux becomes:

$$\frac{d\mathbf{e}_\psi}{dt} = (\mathbf{A}_{22} + L\mathbf{A}_{12})\mathbf{e}_\psi + (\Delta\mathbf{A}_{22} + L\Delta\mathbf{A}_{12})\hat{\boldsymbol{\psi}}_r \quad (14)$$

The Lyapunov function candidate is chosen as:

$$V = \mathbf{e}_\psi^T \mathbf{e}_\psi + \frac{(\Delta\omega)^2}{2\mu\varepsilon}; \mu > 0 \quad (15)$$

The Lyapunov function must be determined in order to assure the convergence of parameter estimation according to the Lyapunov stability theory. The time derivative of Lyapunov function  $V$  can be expressed as:

$$\frac{dV}{dt} = \frac{dV_1}{dt} + \frac{dV_2}{dt} \quad (16)$$

where:

$$\begin{cases} \frac{dV_1}{dt} = \mathbf{z}^T \boldsymbol{\Lambda}^T \mathbf{A}_{12}^{-1} \mathbf{z} \\ \frac{dV_2}{dt} = \hat{\boldsymbol{\psi}}_r^T \mathbf{z}^T \boldsymbol{\Lambda}^T \mathbf{A}_{12}^{-1} \frac{\Delta\omega}{\varepsilon} \mathbf{J} + \frac{dW}{dt} \end{cases}$$

$$\text{and } \boldsymbol{\Lambda} = \mathbf{L} - \varepsilon\mathbf{I}, W = \frac{(\Delta\omega)^2}{2\mu\varepsilon}$$

The condition of (16), being negative definite, will be satisfied if:

$$\begin{cases} V > 0 \\ \frac{dV}{dt} < 0 \Leftrightarrow \frac{dV_1}{dt} < 0 \text{ and } \frac{dV_2}{dt} = 0 \end{cases}$$

The condition  $\frac{dV_1}{dt} < 0$  is satisfied by choosing

$$\Lambda = -\gamma \mathbf{A}_{12}, \gamma > 0 \quad (17)$$

With this assumption, the condition  $\frac{dV_2}{dt} = 0$  gives:

$$\begin{aligned} \frac{dW}{dt} &= \gamma \hat{\psi}_r^T \mathbf{z}^T \frac{\Delta \omega}{\varepsilon} \mathbf{J} = \frac{\Delta \omega}{\mu \varepsilon} \frac{d\hat{\omega}}{dt} \\ \rightarrow \frac{d\hat{\omega}}{dt} &= \mu \gamma \hat{\psi}_r^T \mathbf{z}^T \mathbf{J} \end{aligned} \quad (18)$$

This equation can be written in the following form for the speed estimation:

$$\frac{d\hat{\omega}}{dt} = \mu \gamma k_1 \left[ \hat{\psi}_{r\beta} \text{sign}(i_{s\alpha} - \hat{i}_{s\alpha}) - \hat{\psi}_{r\alpha} \text{sign}(i_{s\beta} - \hat{i}_{s\beta}) \right] \quad (19)$$

To increase the accuracy of the estimated speed, the proportional integral algorithm should be used instead of only integral algorithm, so the speed estimation in (19) can be rewritten as:

$$\hat{\omega} = K_p e_\omega + K_I \int e_\omega dt \quad (20)$$

with:  $e_\omega = \hat{\psi}_{r\beta} \text{sign}(i_{s\alpha} - \hat{i}_{s\alpha}) - \hat{\psi}_{r\alpha} \text{sign}(i_{s\beta} - \hat{i}_{s\beta})$

## 2.2. Rotor flux estimation using SMO

In order to complete the design of the speed control system of the ASM based on rotor field oriented control method, besides the estimation of rotor speed, the value and position of the rotor flux are necessary to be known.

From equation (12) to (14) give:

$$\begin{aligned} [\mathbf{L} - \varepsilon \mathbf{I}]^T &= -\gamma \mathbf{A}_{12} \\ \rightarrow \mathbf{L} &= \left( \varepsilon - \frac{\gamma \sigma_r}{\varepsilon} \right) \mathbf{I} - \frac{\gamma \omega_r}{\varepsilon} \mathbf{J} \end{aligned} \quad (21)$$

or it can be rewritten in short form as:

$$\mathbf{L} = -x \mathbf{I} - y \mathbf{J} \quad (22)$$

To assure the convergence, the condition  $\Lambda \geq -\gamma \mathbf{A}_{12}$  is satisfied by choosing:

$$x = (q-1)\varepsilon + \frac{\gamma \sigma_r}{\varepsilon}, y = q \frac{\gamma \omega_r}{\varepsilon}, q > 0 \quad (23)$$

Then, the matrix  $\mathbf{L}$  can be calculated as:

$$\mathbf{L} = \begin{bmatrix} (1-q)\varepsilon - \frac{\gamma \sigma_r}{\varepsilon} & q \frac{\gamma \omega_r}{\varepsilon} \\ -q \frac{\gamma \omega_r}{\varepsilon} & (1-q)\varepsilon - \frac{\gamma \sigma_r}{\varepsilon} \end{bmatrix} \quad (24)$$

From (3) and (24) the gain matrix  $\mathbf{K}$  of the observer can be written as:

$$\mathbf{K} = \begin{bmatrix} k_1 & 0 \\ 0 & k_1 \\ -k_1 \left[ (1-q)\varepsilon - \frac{\gamma \sigma_r}{\varepsilon} \right] & -k_1 q \frac{\gamma \omega_r}{\varepsilon} \\ k_1 q \frac{\gamma \omega_r}{\varepsilon} & -k_1 \left[ (1-q)\varepsilon - \frac{\gamma \sigma_r}{\varepsilon} \right] \end{bmatrix} \quad (25)$$

Basing on this result the full order rotor flux observer can be derived in Fig. 3

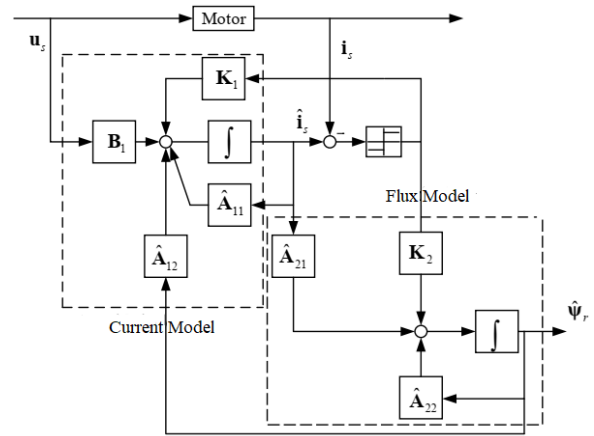


Fig. 3. Full order rotor flux observer

The value of the rotor flux and its position can be calculated in the following equations:

$$\hat{\psi}_r = \sqrt{\hat{\psi}_{r\alpha}^2 + \hat{\psi}_{r\beta}^2}, \hat{\theta}_s = \arctan\left(\frac{\hat{\psi}_{r\beta}}{\hat{\psi}_{r\alpha}}\right) \quad (26)$$

From (12) the system matrix of the error equation of the rotor flux error can be expressed as:

$$\mathbf{A}_{\hat{\psi}} = \mathbf{A}_{22} + \mathbf{L} \mathbf{A}_{12} \quad (27)$$

with:  $\mathbf{L} = -x \mathbf{I} - y \mathbf{J}$ ,  $\mathbf{A}_{12} = c \mathbf{I} - d \mathbf{J}$ ,  $\mathbf{A}_{22} = -\varepsilon \mathbf{A}_{12}$

$$\begin{aligned} \rightarrow \mathbf{A}_{\hat{\psi}} &= \begin{bmatrix} -\varepsilon c - xc - yd & -\varepsilon d + xd - yc \\ \varepsilon d - xd + yc & -\varepsilon c - xc - yd \end{bmatrix} = \\ &= \begin{bmatrix} u & -v \\ v & u \end{bmatrix} \end{aligned} \quad (28)$$

So the polynomial characteristics of the system are:

$$\det(\lambda \mathbf{I} - \mathbf{A}_\psi) = \det \begin{pmatrix} \lambda - u & -v \\ v & \lambda - u \end{pmatrix} = (\lambda - u)^2 + v^2$$

And the root of the equation  $(\lambda - u)^2 + v^2 = 0$  is  $\lambda_{1,2} = u \pm jv$  (29)

Due to  $u = -\epsilon c - xc - yd < 0$  the system is stable because it has two poles located to the left of the virtual axis.

From (24) and (29) we have:

$$\lambda_{1,2} = -q \left\{ \left( \sigma_r + \frac{\gamma}{q} \frac{\sigma_r^2}{\epsilon^2} + \gamma \frac{\omega^2}{\epsilon^2} \right) \pm \left[ \omega + \frac{\sigma_r \omega}{\epsilon^2} \left( \frac{\gamma}{q} - 1 \right) \right] \right\} \quad (30)$$

This relationship demonstrates that the eigenvalues of the error system of the rotor flux are stable. Therefore, adaptive system based on sliding mode in accordance with equation (14) is stable.

The design parameters  $q$  and  $\gamma$  play an important role in improving the accuracy of the estimation. The effect of parameters  $q$  and  $\gamma$  with the different eigenvalues is shown in Fig. 4.

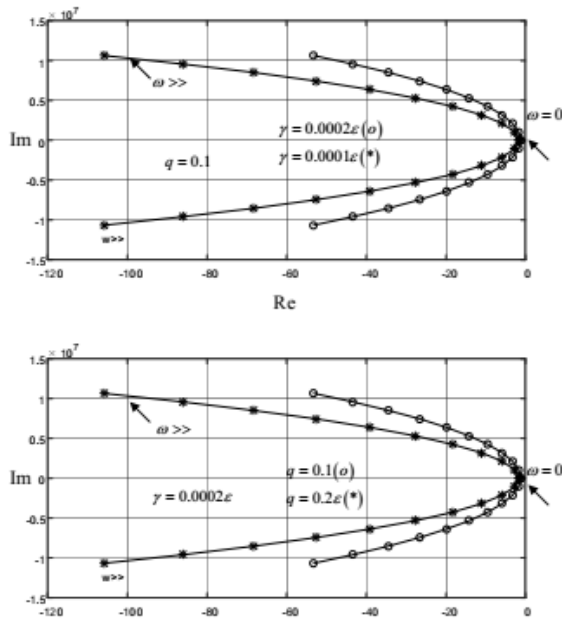


Fig. 4. Eigenvalues of the system

In order to force  $e_\psi$  to zero quickly, the parameters  $q$  and  $\gamma$  (matrix  $\mathbf{L}$ ) should be chosen suitably.

### 3. Results and discussion

#### 3.1 Simulation results

To verify the proposed design method, the speed control system of the ASM using a sliding mode observer is built on the Matlab / Simulink. The simulation results are shown in Figures 5, 6, 7 and 8.

Table 1. Parameters of 1LA7096

Parameter	Symbol	Value
Nominal power	$P_{dm}$	2.2 kW
Nominal torque	$M_{dm}$	7.3 Nm
Nominal phase current	$I_{dm}$	4.7 A
Nominal phase voltage	$U_{dm}$	400 V
Nominal frequency	$f_{dm}$	50 Hz
Pole pair	$p$	1
Stator resistance	$R_s$	1.99 $\Omega$
Rotor resistance	$R_r$	1.99 $\Omega$
Magnetizing inductance	$L_m$	0.37 H
Rotor leakage inductance	$L_{\sigma r}$	0.01 H
Stator leakage inductance	$L_{\sigma s}$	0.01 H
Nominal speed	$n_{dm}$	2880 rpm
Moment of inertia	$J$	0.0018 Kg.

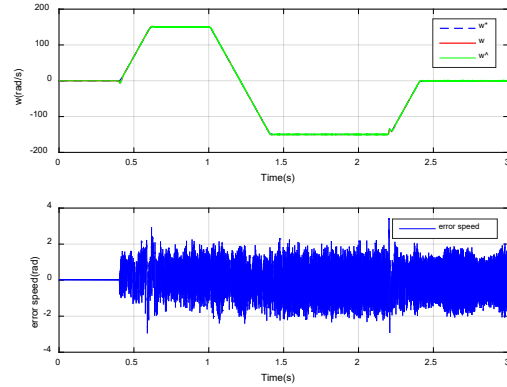


Fig. 5 Speed response and error

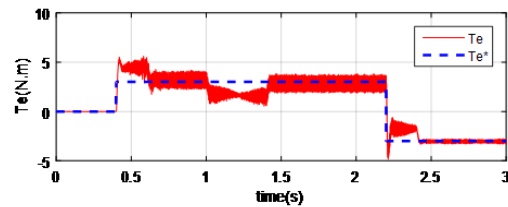


Fig. 6 Moment response

Figs. 5 and 6 show the responses of speed and moment of the ASM at the start and reversal. At the

time of 0.4s the ASM starts to run to 150 rad/s when the load is set to 3Nm. At the time of 1s, the ASM is reversed to -150 rad/s. The ASM is stopped at 2.2s. For more detail, the three-phase current is illustrated in Fig. 7. Obviously, the estimated speed always reaches the reference speed in all working conditions. At the acceleration, deceleration and reversal, there is overshoot, however the maximum error is about 1,5 rad/s (1%).

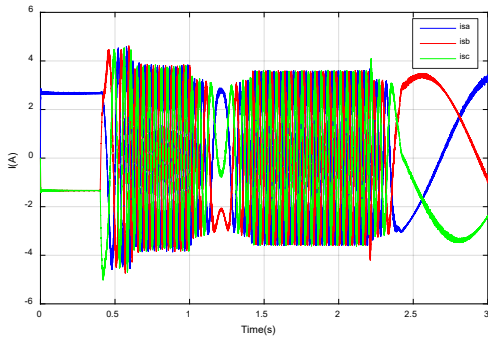


Fig. 7 Response of three-phase current

### 3.2 Experimental results

To increase the reliability of the proposed estimation method, It is also implemented on the test bed which is shown in Fig. 8

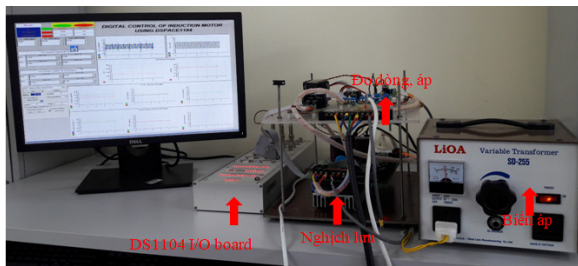


Fig. 8 Test bed of the ASM with DS1104

Experimental model of asynchronous motor drives uses two motors which are rigidly connected together. The Siemens ASM 1LA7096, nominal power of 2.2 KW, is experimental motor and the Siemens PMSM 1FK7080 combined with Sinamics S120 inverter play a role of load. The control hardware of the ASM drives is based on a dSPACE DS1104 board dedicated to the control of electrical drives. The DS1104 reads the rotor angle position and speed from the encoder via an encoder interface. Two motor phase currents are sensed, rescaled, and converted to digital values via the A/D converters. The DS1104 then calculates reference currents and sends its commands to the three-phase inverter boards. The ASM is supplied by voltage source three-phase inverter with a switching frequency of 8 kHz. Experimental results are described in detail in Figures 9, 10 and 11.

Results from Figures 9 and 10 show that the estimated speed is always close to the measured speed in all operating modes such as start, stop and reversal, although in the transient mode there is a deviation in estimated and measured speeds as shown in Figure 11. However, this deviation (maximum of about 9% at 1.2s) is in acceptable range. Thus, the experimental results are quite similar to the above simulation results

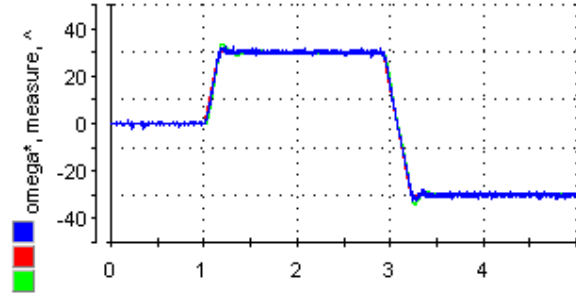


Fig. 9 Response of speed

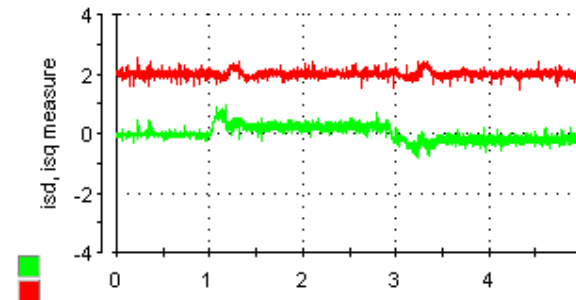


Fig. 10 Response of  $i_{sd}$  and  $i_{sq}$  currents

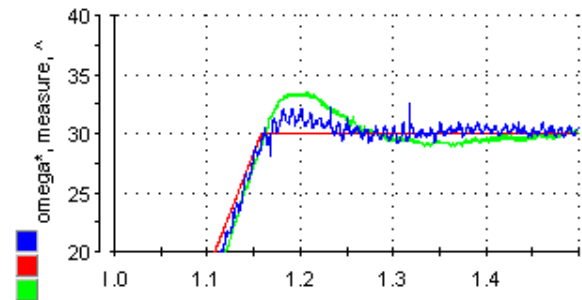


Fig. 11 Response of estimated and measured speed at acceleration (in detail)

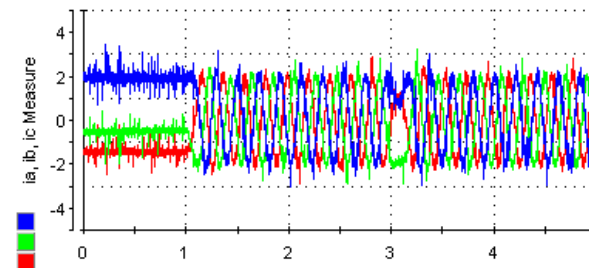


Fig. 12 Response of three-phase current

#### 4. Conclusion

The paper introduced the method of estimating the rotor speed, flux and its position to serve for the sensorless speed control of an asynchronous motor. The simulation and experimental results show that the estimated results always follow the measured ones in all operating modes. The ASM drives can work stably and highly accurately without any speed sensor.

#### Acknowledgments

This research is funded in part by the Ministry of Science and Technology through the project "Research, design and manufacture of three-phase AC servo drives", Code 44 / 16- ĐTĐL.CN-CNC.

#### References

- [1] Zineb Kandoussi, Boulghasoul Zakaria, Abdelhadi Elbacha, Tajer Abdelouahed; Sensorless control of induction motor drives using an improved MRAS observer; *Journal of Electrical Engineering and Technology*. Vol. 12. (2017) pp. 1456-1470..
- [2] Danyang Bao, Hong Wang, Xiaojie Wang and Chaoruo Zhang; Sensorless Speed Control Based on the Improved Q-MRAS Method for Induction Motor Drives; *Journal of Energies*. Vol. 11 (2018), No. 235. pp. 1-16.
- [3] Arif Iqbal, Mohammed Husain; MRAS based Sensorless Control of Induction Motor based on Rotor Flux. (2018) 152-155.
- [4] Francesco Alonge, Filippo D'Ippolito, Antonino Sferlazza; Sensorless Control of Induction-Motor Drive Based on Robust Kalman Filter and Adaptive Speed Estimation; *IEEE Transactions on Industrial Electronics*. Vol. 61 , Issue: 3 , (2014) pp. 1444 - 1453.
- [5] Francesco Alonge, Filippo D'Ippolito Adriano Fagiolini, Antonino Sferlazza;. Extended complex Kalman filter for sensorless control of an induction motor; *Journal of Control Engineering Practice*. Volume 27, (2014) pp. 1-10.
- [6] Imane Ghlib, Youcef Messlem, Abdelmadjid Gouchiche, Chedjara Zakaria; Neural Adaptive Kalman Filter for Sensorless Vector Control of Induction Motor; *International Journal of Power Electronics and Drive Systems (IJPEDS)*. Vol. 8. (2017) pp. 1841-1851.
- [7] M. Zerikat, A. Mechernene, S. Chekroun; High-performance sensorless vector control of induction motor drives using artificial intelligent technique; *International Transactions on Electrical Energy Systems*. Volume21, Issue1, (2011) pp. 787-800
- [8] Abolfazl Halvaei Niasar, Hossein Rahimi Khoei; Sensorless Direct Power Control of Induction Motor Drive Using Artificial Neural Network; *Advances in Artificial Neural Systems Volume 2015*. pp. 1-9
- [9] Pranav Pradip Sonawane, 2MRS. S. D. Joshi. Sensorless speed control of induction motor by artificial neural network. *International Journal of Industrial Electronics and Electrical Engineering*. Volume-5, Issue-2, (2017) pp. 44-48
- [10] Aurora, Claudio & Ferrara, Antonella.. A sliding mode observer for sensorless induction motor speed regulation. *Int. J. Systems Science*. Vol. 38, (2007) pp. 913-929
- [11] Kari, Mohammed Zakaria; Mechernene, Abdelkader; Meliani, Sidi Mohammed. Sensorless Drive Systems for Induction Motors using a Sliding Mode Observer. *Electrotehnica, Electronica, Automatica: EEA; Bucharest* Vol. 66, Iss. 2, (2018) pp. 61-68.
- [12] Dong Chau, Vo Hau, Cong Tran Thinh & Brandstetter Pavel, Simonik Petr.; Application of Sensorless Sliding Mode Observer in Control of Induction Motor Drive; *Advances in Electrical and Electronic Engineering*. Vol. 15, No. 5, (2018) pp.747-753 .
- [13] Vadim I. Utkin: *Sliding Modes in Control Optimization*, Springer-Verlag, 1992, ISBN 3-540-53516-0 or 0-387-53516-0.
- [14] Quang N. P., Joerg-Andreas Dittrich (2015); *Vector Control of Three-Phase AC Machines*; Springer Verlag GmbH.
- [15] Quang N.P. (2008); *Matlab và Simulink dành cho kỹ sư điều khiển tự động*; NXB Khoa học và Kỹ Thuật..